

SPIN COATED TANTALUM-TIN OXIDE THIN FILM PREPARED USING TANTALUM-TIN ACETYLACETONATE AS PRECURSOR

Olawale Simbo ADESANLU¹, Marcus Adebola ELERUJA¹, Victor ADEDEJI², Oladepo FASAKIN¹, Bolutife OLOFINJANA^{1*}, Eusebis Ikechukwu OBIAJUNWA³, Ezekiel Oladele Bolarinwa AJAYI¹

¹Department of Physics and Engineering Physics, Obafemi Awolowo University, Ile-Ife, 220005, Nigeria

²Department of Chemistry and Physics, Elizabeth City State University, Elizabeth City, NC, USA

³Center for Energy Research and Development, Obafemi Awolowo University, Ile-Ife, Nigeria

Abstract

A single source precursor, tantalum tin acetylacetonate was prepared and characterized by Fourier transform infrared (FTIR) spectroscopy. Tantalum tin oxide thin film was deposited on ITO coated glass substrate through spin coating of the single source precursor solution and annealed at a temperature of 420 °C. The deposited film was characterized using Rutherford backscattering spectroscopy (RBS), scanning electron microscopy (SEM), X-ray diffractometry (XRD), optical absorption spectroscopy, and four point probe technique. RBS analysis showed that the film have a stoichiometry of $Ta_{0.2}Sn_{0.8}O_2$ and thickness of 8.225 nm. SEM micrograph of the film revealed closely packed grains which are well distributed over the entire substrate while the XRD indicated strong reflections from planes that correspond to both tetragonal rutile SnO_2 and Ta_2O_5 structures. The absorption behavior of the deposited thin film was relatively stable under different temperature with direct optical band gap between 3.44 and 3.54 eV. The resistivity was found to be of the order of $10^{-4} \Omega\text{-cm}$.

Keywords: Spin coating, precursor, tantalum tin acetylacetonate, tantalum tin oxide, thin film, characterization

Introduction

Transparent conducting oxide (TCO) materials offer broad range of outstanding features. They are wide band gap materials (≥ 3 eV) whose behavior and characteristics are highly influenced by the oxidation state (i.e. stoichiometry) and sometimes the nature as well as the quantity of other element trapped in the material [1, 2]. More importantly, they have high chemical and mechanical stability coupled with absence of toxicity and abundance in nature [3, 4]. In addition to all these, TCO materials have interesting combination of high transparency and excellent electrical conductivity [5-8]. Many of these features have been applied in various technological applications ever since the material was produced in micro-or-nano-crystalline form, exhibiting high surface-to-volume ratio and short solid state diffusion paths. For instance, TCO thin films are essential components of various devices that have become part of our everyday lives. They are used in transparent conducting electrodes (TCE) as flat panel display, solar cells, light emitting diodes (LEDs), flexible liquid crystal display, gas sensors, electrochromic devices, heat reflecting coatings, architectural window coatings, laser damage resistant coatings, catalytic support materials [1, 9-13], among others.

Most of the TCO thin film materials that are famous nowadays are based on In_2O_3 , SnO_2 and ZnO . Among these various TCO thin films, SnO_2 seems to be one of most versatile. This is

*Corresponding author: olofinb@oauife.edu.ng, olofinbolu@gmail.com

because SnO₂ has stable physical, chemical and thermal properties at high temperatures and in chemical environments. Generally, SnO₂ with rutile crystal structure is an n-type material with resistivity in the range of 10⁻² to 10⁻³ Ω-cm. However in most practical applications, SnO₂ thin films is usually doped or alloyed with other TCO thin films in order to reduce the resistivity. Such dopant or other TCO thin film materials can then supply excess carriers to the SnO₂ lattice and form oxygen vacancy during deposition process. Both mechanisms generate the needed free electrons necessary for increase in the film conductivity.

There are other varieties of TCO thin films that have also shown good electrical conductivity. Such TCO thin films include doped In₂O₃, ZnO, CdO and combination of these oxides. Among these, Sn-doped-In₂O₃ popularly called indium tin oxide (ITO) is widely used. However, ITO seems to have some drawbacks. For instance, ITO is sensitive to harsh environmental condition which can degrade the electrical conductivity of the film. In addition, expansion coefficient mismatch between ITO film and substrate creates stress/strain on the film when subjected to high and fluctuating temperature which can lead to micro-cracks and consequently damage the film [14]. It has also been suggested that ITO is at its maximum capability in high density application [15]. There is also the issue of scarcity of indium which has led to high cost of ITO. Due to all these drawbacks, alternative TCO thin film materials with improved electrical and optical properties which may contribute to better device performances even in harsh environmental conditions are sought after.

There have been several studies to explore new thin film materials as suitable alternatives to ITO thin films [3, 15-17]. Interestingly, some of these thin film materials are based on SnO₂ system either as doped-SnO₂ or combination of SnO₂ with others TCOs. Various dopants such as fluorine, antimony, molybdenum and tantalum have been shown to improve electrical and optical properties of SnO₂ thin films [2, 5, 7, 18-20]. Low electrical resistivity and good optical performance have also been achieved by other SnO₂ based systems such as ZnO-In₂O₃-SnO₂, ZnO-SnO₂ thin films [3, 15, 21]. Among many doping materials, tantalum seems to be the most promising [22-24]. This is because tantalum tin oxide (TTO) thin films have shown promising properties. In addition, the radius of Ta⁵⁺ from Ta₂O₅ is similar to that of Sn²⁺ and only a small amount of lattice deformation will occur even if high concentration of Ta⁵⁺ is introduced. With abundance of SnO₂ and Ta₂O₅ in nature, TTO thin films will be expected to be cheap. Their properties can be tailored to withstand harsh environmental conditions with the advantage of good thermal stability.

TTO thin films have been grown by various techniques. This includes chemical vapor deposition [5, 12], pulse laser deposition [22, 23], sputtering [7, 24], among others, with resistivity as low as the order of 10⁻³ to 10⁻⁴ Ω-cm reported. Increase in carrier concentration was reported to be the most influential factor for the decrease in resistivity. Carrier concentration increases because of the substitution of Ta ions into Sn anion sites which act as an n-type dopant that supplies free electrons. In addition, Lee et al. (2001) [12] reported that at low temperature region, the carrier concentration tends to increase with temperature. This was explained as hopping conduction through impurity states presumably oxygen vacancy states within the bands. An appreciable enhancement of mobility which is related to microstructural improvement was also reported by Kim et al. (2002) [5] and was stated to be the reason for decrease in resistivity. The improvement in mobility was believed to come from the lattice alignment with less mosaicity of grains leading to reduction in the scattering of electrons at grain boundaries and adjacent lattice planes.

Most studies that have been reported on TTO thin films were films prepared using complex techniques with multi-source precursor components. Motivated by this, the main

objectives of the present study are to: prepare and characterize a single source precursor for TTO thin film, deposit TTO thin film from the prepared precursor using a simple technique and then characterize the thin film in order to study its properties. The use of single source precursor provides a novel approach with benefits such as reduction of the number of parameters controlling the stoichiometry and properties of the film. In this work, TTO thin film was deposited on ITO coated glass substrate from single source precursor using spin coating technique. Spin coating technique is a preparative method well suited to large scale production which is simple and cost effective. The precursor was characterized by Fourier transform infrared (FTIR) spectroscopy while the compositional, morphological, structural, optical and electrical studies of the film were done using Rutherford backscattering spectroscopy (RBS), scanning electron microscopy (SEM), X-ray diffraction (XRD), UV-visible spectroscopy and four point probe method of electrical resistivity respectively.

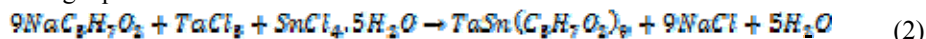
Materials and Methods

Preparation and characterization of the precursor

The liquid source precursor used in this work was prepared using a modification of the method earlier reported by Mordi et al. (2009) [25]. This method has also been extended to cover solid precursors for the preparation of ternary metal oxide thin films [26, 27]. Chemical reagents used are 2, 4-pentanedione (acetylacetonate), sodium hydroxide (NaOH), tantalum pentachloride (TaCl_5), tin (IV) chloride hydrate ($\text{SnCl}_4 \cdot 5\text{H}_2\text{O}$) and methanol. 40 mL of acetylacetonate was added slowly to 16.0 g (0.3 mol) of NaOH (dissolved in 150 mL of water) and kept at a temperature below 14°C to yield a yellow solution of sodium acetylacetonate ($\text{NaC}_5\text{H}_7\text{O}_2$). The reaction can be depicted as:



35.82 g (0.10 mol) of TaCl_5 was dissolved in 50 mL of cold methanol; 35.05 g of $\text{SnCl}_4 \cdot 5\text{H}_2\text{O}$ was also dissolved in 50 mL of cold methanol. The solutions of TaCl_5 and $\text{SnCl}_4 \cdot 5\text{H}_2\text{O}$ in methanol was simultaneously introduced into the yellow solution of $\text{NaC}_5\text{H}_7\text{O}_2$ and vigorously stirred. A white precipitate of tantalum tin acetylacetonate was obtained. The resulting white precipitate was filtered in a large Buchner funnel and washed with 500 mL of distilled water. The filtrate was then dried in an oven maintained at 60°C . The reaction scheme is represented by the following equation:



The solid tantalum tin acetylacetonate was grounded into fine powder and characterized by Fourier Transform Infrared (FTIR) spectroscopy using a Shimadzu FTIR-8400 S spectrophotometer. The transmission spectrum was measured in KBr at normal incidence angle over the range of 4000 and 500 cm^{-1} in ambient room temperature. The fine powder of tantalum tin acetylacetonate was then dissolved in cold methanol to obtain a clear solution.

Deposition and characterization of thin film

The tantalum tin oxide thin film was deposited using spin coating technique. It is a technique which uses a liquid source precursor for thin film coating of the desired material on a substrate. The obtained solid tantalum tin acetylacetonate was grounded into fine powder and dissolved in cold methanol which was then spin coated on ITO glass substrate at a speed of 850 rpm. This was then annealed at a temperature of 420°C for 2 hours in oxygen environment.

Rutherford backscattering spectroscopy (RBS) was used to determine elemental composition, stoichiometry and thickness the thin film. The RBS facility is a 1.7 MeV Tandem accelerator of IBM geometry in which the incident beam, surface normal and detected beam are all co-planar. The incident beam was He⁺ with a current of 3.8 nA and integrated beam dose of 10.0 μC. The silicon detector solid angle was 0.833 msr with a resolution of 12 keV. SIMNRA software was used to analyze the spectrum that was extracted from the silicon detector.

The surface morphology of the film was obtained using Zeiss DSM 940 scanning electron microscope. The electron beam of the SEM was 0.1 keV-30 keV with nominal resolution of 1 nm at 10 keV. Secondary electrons were acquired to produce the SEM micrograph under 10 kV accelerating voltage with a working distance of 10 mm.

X-ray diffraction (XRD) analysis of the thin film was carried out using Radicon X-ray mini diffractometer of model MD-10. The diffractometer is equipped with a high voltage source of 25 kV which deliver Cu-K_α radiation of wavelength 1.5418 nm. The diffraction angle 2θ, ranged from 20° to 60°. Chemical phase identification was also performed using a computer based system with standard powder diffraction file (PDF) embedded in the machine. This was done by comparing our diffraction data with a data base maintained by the International Center for Diffraction Data (ICDD).

Optical measurements constitute one of the most direct and probably one of the simplest approaches for probing the band structure and ultimately the suitability of the deposited film for device applications. In order to study the optical behavior of the thin film, the optical absorbance of the film was investigated using Jenway UV-Visible spectrophotometer (Model 26405). All measurements were made at temperatures ranging between 25°C and 60°C in the wavelength range of 200 to 1100 nm at interval of 5 nm. Standardization was first done by placing plain substrate in the sample and reference beam position, thus having plain substrate against substrate plain, after which the coated substrate was then placed in the sample position.

The electrical characterization of the film was investigated using four point probe technique. The four point collinear configuration was employed for the operation of Keithley Four-Point Probe Machine (Model 2400). Silver paste was deposited at each of the four points for ohmic contact. Keithley 2400 source meter with Rolls and Keener probes was used for the current-voltage measurements. The two outer probes were used to source current while the two inner probes source the resulting voltage drop across the thin film.

Results and Discussion

FTIR analysis of the precursor

Figure 1 shows the FTIR spectrum obtained for the solid tantalum tin acetylacetonate in KBr. The FTIR was used to identify the functional groups present in the solid tantalum tin acetylacetonate. A close observation of the spectrum showed that the precursor exhibits basic absorption bands between 4000 cm⁻¹ and 500 cm⁻¹. Generally, all the enol from all β-diketones exhibits extremely broad bands in the frequency range 3500 – 2200 cm⁻¹ [28]. The spectrum shows O-H stretch vibration at 3416.05 cm⁻¹ which can be attributed to alcohol functional group. The appearance of this band may be as a result of the methanol used as solvent for dissolving chemical reagents used in preparing the precursor. The band at 3109.35 cm⁻¹ can be assigned to olefinic CH stretching mode and the 3005.20 cm⁻¹ band to plane symmetric CH₃/CD₃ stretch. The band at 2924.18 cm⁻¹ can be as a result of CH₃ symmetric stretching of methyl groups while the out of plane asymmetric CH₃/CD₃ can be as a result of the bands at 2476.68, 2362.88 and 2137.20 cm⁻¹. The weak band at 1961.67 cm⁻¹ corresponds to OD

stretching. Other bands which are observed in the region between 1700 and 1000 cm^{-1} are in relation to the enol ring modes. Such bands can be attributed to C O, C-O, C C, C-C stretching and the OH bending modes. The bands at 1618.33 and 1539.55 cm^{-1} belong to C C-O + C-CH₃ mode. The band at 1423.51 cm^{-1} can be assigned to asymmetric C-C, C-O stretch while band at 1340.57 cm^{-1} can be attribute to C-O, C O stretch and δ_{OH} . Bands at 1282.71 and 1024.24 cm^{-1} are assigned to C-CH₃ C-C CC stretch and δ_{OH} . Bands 937.44 and 810.13 cm^{-1} can be as result of δ_{CH} while bands below 700 cm^{-1} can be attributed to metal-oxygen. Our assignment of bands is in agreement with that of Tayyari and Milani-nejad (2000) [28] for β -diketones. This indicated the presence of acetylacetonate in the prepared precursor.

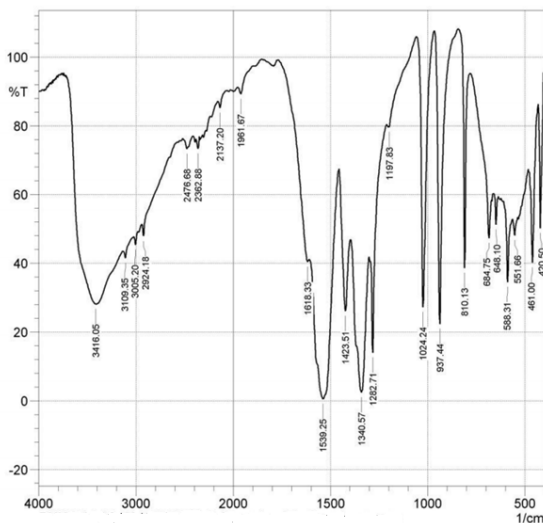


Fig.1. FTIR spectrum of tantalum tin acetylacetonate.

Elemental composition and thickness of the thin film

Elemental composition and thickness analysis was carried out using RBS. The SIMNRA code (version 6.06) was used for fitting the simulated data over the experimental data. The information regarding the stoichiometry and areal concentration of the film was also extracted. The RBS spectrum is shown in Figure 2. The simulated spectrum is based on hypothetical data in the database of the analyzing software for the elements envisaged. The real data from the sample are then characterized based on the simulated spectrum. Each element detected is matched with the database for identification while the overall concentration of the detected elements gives rise to the thickness of the film. The expected elements were detected with a stoichiometry of $\text{Ta}_{0.2}\text{Sn}_{0.8}\text{O}_2$. The higher percentage of oxygen in the composition can be traced to the fact that the film was annealed in oxygen environment at 420 $^{\circ}\text{C}$ for 2 hours. A thickness value of 8.225 nm was also estimated from the RBS data.

Surface morphology of the thin film

The micrograph of the film is shown in Figure 3. It can be seen that the film have closely packed grains which are well distributed over the entire substrate suggesting that the film adhere well to the substrate without any crack. This may be attributed to the volume expansion during the formation of formation of the film [27, 29]. The processes involved in the growth of the film may be a feature of stronger interaction between deposited grains of the film than that of the film and the substrate, indicating the effectiveness of spin coating technique (used in this

work) in the production of crystalline film. Although the grains are evenly distributed across the substrate, the shape and size of the grains are not well defined.

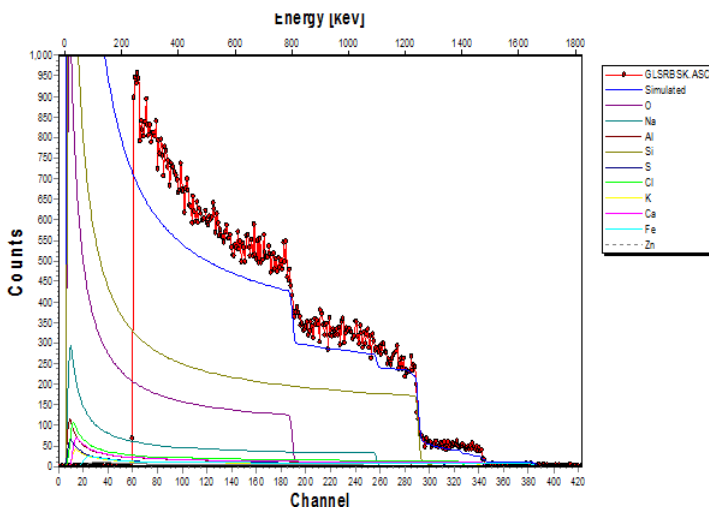


Fig. 2. RBS spectrum of Ta-Sn-O thin film.

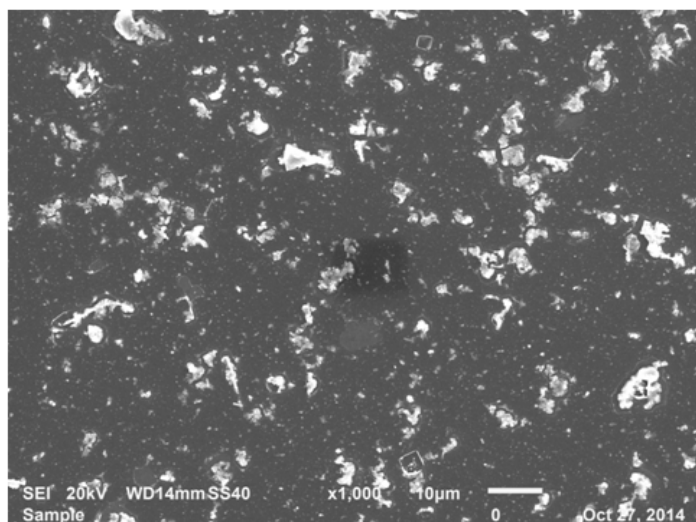


Fig. 3. SEM micrograph of Ta-Sn-O thin film.

Crystal structure

The nature and extent of crystallinity of thin films can be understood by studying its structural properties using XRD technique. In this study XRD analysis of the thin film was carried out using Radicon X-ray mini diffractometer of model MD-10. The diffraction pattern of TTO thin film deposited on ITO glass substrate is presented in Figure 4. It reveals seven characteristic peaks that can be attributed to ITO, SnO₂ and Ta₂O₅ crystals. Major peaks of ITO occurred at $2\theta = 30.52^\circ, 35.5^\circ$ and 51° which correspond to reflections from planes (222), (400) and (441) respectively (JCPDS Card No: 89-4597). The (222) plane of ITO has always been the strongest peak for ITO [30] and it is also what was observed in our case. The peaks at

$2\theta = 31^\circ$ and 51.75° correspond to reflections from planes of SnO_2 tetragonal rutile structure (JCPDS Card No: 88-0287). The remaining peaks at $2\theta = 21.5^\circ$ and 50.5° correspond to reflections from planes (001) and (110) of Ta_2O_5 crystal structure (JCPDS Card No: 71-0639). There seem to be ambiguity as to actual phase of the Ta_2O_5 structure. This ambiguity occurs because the spectra of the two phases (α - and β - phase) of the Ta_2O_5 structure are too similar to allow distinction between them on the basis of XRD alone [31]. Strong reflections from planes which correspond to both SnO_2 and Ta_2O_5 indicated that the deposited film is polycrystalline in nature.

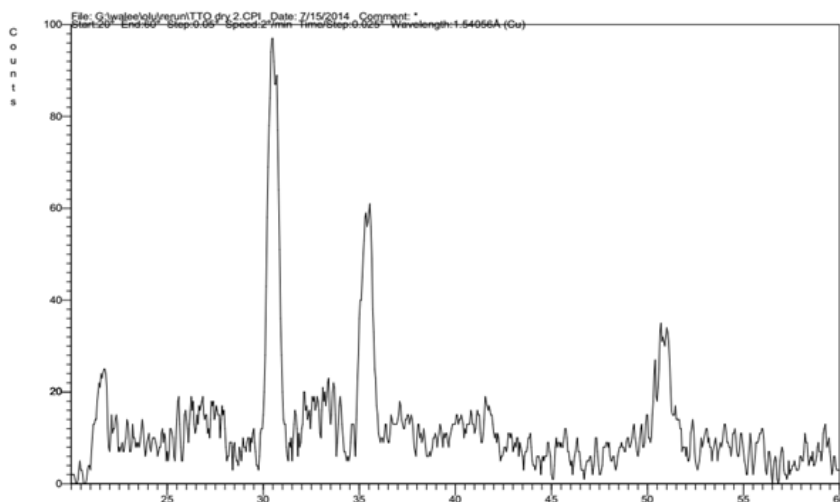


Fig. 4. XRD pattern of Ta-Sn-O thin film.

Optical studies of the thin film

In order to study the optical properties of the deposited film under different environmental conditions, the UV-Visible spectrum of the deposited film was obtained at temperatures ranging between 25 and 60 °C. The spectrum is a plot of absorbance against wavelength at normal incidence. Figure 5 shows the UV-Visible absorbance spectrum acquired in the wavelength range of 330-800 nm. From the Figure, it can be seen that, the variation of absorbance against wavelength at all temperatures follow the same trend. This goes to show that the absorption behavior of the deposited thin film is relatively stable under different temperature. The absorption intensities dropped rapidly from the maximum values which occurred around 331 nm. This was followed by gradual decrease up to about 665 nm and a nearly constant value between 670 and 800 nm. The strong absorption around 330-355 nm can be attributed to inter-band transition from filled oxide valence band to the empty conduction band [32]. In addition, the presence of defects such as oxygen vacancy can also result in high absorption [33]. A sharp absorption edge was observed around 350-360 nm. Well defined absorption edges indicate a good quality film in which the ternary compound comprise of a solid solution [34]. In our own case, this is because high degree of crystallization of the film was obtained during deposition as can be seen in the XRD spectrum.

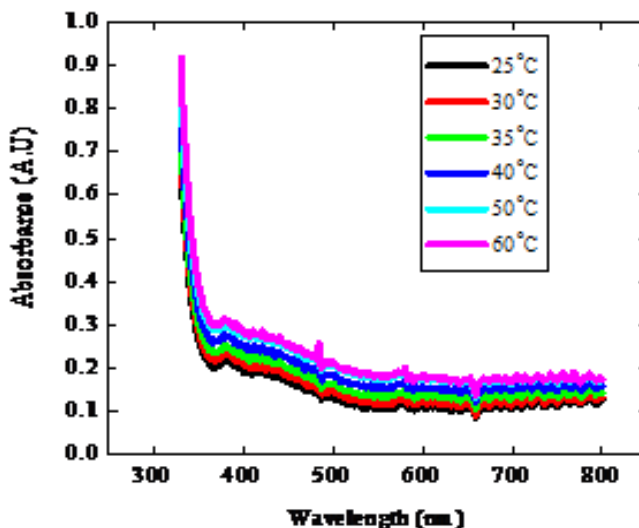


Fig 5. Absorbance against wavelength of Ta-Sn-O thin film.

The absorption coefficient, α of the deposited TTO thin film was estimated from absorbance data corresponding to different wavelength at various temperature using the following relation

$$\alpha = \frac{1}{x} \ln\left(\frac{1}{T}\right) \tag{1}$$

where x is the thickness of the same (from RBS) and T is the transmittance given by

$$T = 10^{-A} \tag{2}$$

and A is absorbance at specific wavelength. The spectra dependence of absorption coefficient of the photon energy helps to understand the band structure and electronic transition(s) involved in the absorption process. The dependence of absorption coefficient on photon energy can be obtained using the time-dependent perturbation theory. In crystalline or amorphous materials, the involved optical transition at high values of absorption coefficient ($\alpha \geq 10^4$) above the exponential tail follows a power law of the form

$$\alpha = C(h\nu - E_g)^n \tag{3}$$

where $h\nu$ is the energy of the incident photon; h Planck's constant, ν frequency of the incident radiation; C , an energy independent constant and is a measure of the steepness of band tail density of states (Urbach region); E_g is the optical band gap; and n is an index which characterize the type of optical transition involved in the photon absorption process. The index n can take values equal to 0.5, 1.5, 2, and 3 for allowed direct, forbidden direct, allowed indirect and forbidden indirect transitions respectively. The spectra dependence of absorption coefficient, α observed in the photon energy range (not shown here) has one slope. This indicates the presence of direct optical transition in the deposited TTO thin film. Figure 6 shows the plot of absorption coefficient square α^2 against photon energy $h\nu$. The direct optical band gap of the TTO thin film was calculated using the intercept of the linear part of the curve extrapolated to zero along the energy axis. The direct optical band gap values obtained at various temperatures for the TTO thin film is presented in Table 1. It is known that the deposition temperature normally affect the value of optical band gap of most thin film materials. For instance in the work of Raghupathin et al. (2015) [6], the direct band gap of SnO₂ was found to increase from 3.76 to 3.97 eV as the deposition temperature increases. The

widening of the band gap which was termed Burstein-Moss shift and attributed to the partial filling of the conduction band, which results in a blocking of the lowest states. A decrease from 4.44 eV to 4.25 eV with increase in substrate temperature from 303 to 937 K was also observed for tantalum oxide thin films [33]. The decrease in optical band gap with increase in substrate temperature was attributed to the improvement in packing density and crystallinity of the film. Generally, in semiconducting materials, optical band gaps are influenced by defects, residual stress, impurities and grain boundary disorder [35]. Tensile strains is also known to result in decrease in band gaps due to extended lattice while compressional strains enhance the optical band gaps due to lattice compression [33]. In our case, the direct optical band gaps obtained at different temperature are relatively stable between 3.44 and 3.54 eV indicating that such stress and strains are probably absent. This implies that the deposited TTO thin film can operate under different temperature without significant change in the band gap.

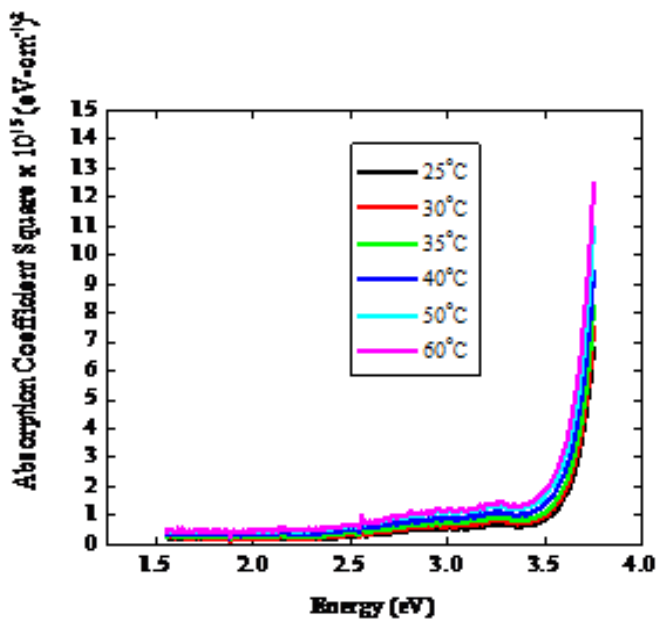


Fig. 6. The plot of α^2 versus energy at various temperatures.

Electrical characterization

Four point probe technique was used to study the electrical property of the deposited TTO thin film. The I-V characteristic of the film at temperatures ranging between 25 and 60°C was measured several times with current and voltage drop point swapped in order to minimize error. The resistance $R_{12,34}$ can be defined as

$$R_{12,34} = \frac{V_{34}}{I_{12}} \tag{4}$$

where current I_{12} enters the sample through contact 1 and leaves through contact 2 and V_{34} is the voltage difference between contacts 3 and 4 ($V_4 - V_3$). Similarly,

$$R_{34,12} = \frac{V_{12}}{I_{34}} \tag{5}$$

The resistivity of the film was obtained using the expression [36],

$$\rho = \frac{\pi t}{\ln(2)} \frac{(R_{12,34} + R_{34,12})}{2} \tag{6}$$

where t is the thickness of the film (from RBS) and F the van der Pauw correction factor which is a function of the ratio

$$R_T = \frac{R_{1234}}{R_{2341}} \tag{7}$$

satisfying the relation

$$\frac{R_T - 1}{R_T + 1} = \frac{F}{\ln(2)} \operatorname{arccosh} \left(\frac{\sin \left(\frac{\ln(2)}{F} \right)}{2} \right) \tag{8}$$

The resistivity of the film at different temperatures is presented in Table 1. The resistivity value obtained in this work is of the same order of magnitude with what was obtained from other TTO thin films and doped-SnO₂ thin films [4, 5, 11, 15, 37]. It can also be seen that the resistivity is approximately invariant under temperature. This implies that the deposited TTO thin film exhibited metallic behavior within the low temperature range. Such behavior was also observed by Lin et al. (2013) [2] and Lee et al. (2001) [12]. Compared with the resistivity of undoped-SnO₂ thin films, which is of the order of 10⁻² to 10⁻³ Ω-cm, there is an improvement in the resistivity of the deposited TTO thin film. An improvement in the resistivity value of the deposited TTO thin film suggested that Ta atom played an important role. From the well-known relationship $\rho = (nq\mu)^{-1}$, in which resistivity is inversely related to carrier concentration and mobility, the carrier concentration and mobility are the main factors controlling the resistivity. However, it has been reported by Lee et al. (2001) [12] that the carrier concentration is the main factor controlling resistivity in TTO thin films. Doping with Ta atom could supply excess carriers to the lattice and form oxygen vacancies which are also source of charge carriers. Both the Ta dopant and the oxygen vacancies generate free electrons which from the equation above reduces the resistivity. Another possibility is that in the TTO thin film, the Ta atoms may diffuse into SnO₂ matrix. Due to difference in their grain sizes, the diffusion of Ta atoms in SnO₂ matrix can cause an increase in free interstitial spaces leading to increase in the mobility of the valence electrons in these free spaces [8]. From the resistivity equation, increase in mobility automatically causes decrease in resistivity.

Table 1: Band gap and resistivity values for the deposited TTO thin film.

| Temperature (°C) | Band gap (eV) | Resistivity x 10 ⁻⁴ (Ω-cm) |
|------------------|---------------|---------------------------------------|
| 25 | 3.44 | 3.49 |
| 30 | 3.47 | 3.48 |
| 35 | 3.48 | 3.53 |
| 40 | 3.54 | 3.51 |
| 50 | 3.52 | 3.52 |
| 60 | 3.46 | 3.50 |

Conclusion

Tantalum tin acetylacetonate was prepared as a single source precursor from commercial reagents and characterized using FTIR. To the best of our knowledge this has not been hitherto used as a precursor in any technique employed in the preparation of TTO thin films. Spin coating of the precursor solution in methanol yielded TTO thin film after annealing at a temperature of 420°C for 2 hours in oxygen environment. Compositional and thickness studies with RBS gave a stoichiometry of Ta_{0.2}Sn_{0.8}O₂ and thickness of 8.225 nm. The morphology of

the film showed that the film have closely packed grains which are well distributed over the entire substrate without definite shape. XRD showed strong reflections from planes which correspond to both tetragonal rutile SnO_2 and Ta_2O_5 structures and thus indicated that the deposited TTO film is polycrystalline in nature. Optical absorption measurements at temperatures between 25 and 60 °C indicated that the variation of absorbance against wavelength at all temperatures follow the same trend while the direct optical band gap obtained at different temperatures was relatively stable between 3.44 and 3.54 eV. Electrical characterization of the deposited TTO thin film showed that the resistivity was approximately invariant under temperature with order of magnitude of 10^{-4} Ω -cm.

It is believed that the deposition of TTO thin film from single source precursor using spin coating technique provides another method of preparing TTO thin film with the advantage of large area deposition. A simple and cost effective method suitable for large scale production of tantalum tin oxide thin film has been established.

References

- [1] G. Kiriakidis, H. Ouacha, N. Katsarakis, *InO_x nanostructured thin films: Electrical and sensing characterization*, **Reviews on Advanced Materials Science**, **4**, 2001, pp. 32-40.
- [2] Y.Y. Lin, H.Y. Lee, C.S. Ku, L.W. Chou, A.T. Wu, *Bandgap narrowing in high dopant tin oxide degenerate thin film produced by atmosphere pressure chemical vapour deposition*, **Applied Physics Letters**, **102**, 2013, pp. 1-5.
- [3] P. Jain, D. Bhandari, Y.K. Vijay, *Study of post annealing influence on structural, chemical and electrical properties of ZTO thin films*, **Journal of Alloys and Compounds**, **509**, 2011, pp.3541-3546.
- [4] X.Q. Pan, L. Fu, *Tin oxide thin films grown on the (10-12) sapphire substrate*, **Journal of Electroceramics**, **7**, 2001, pp. 35-46.
- [5] Y.W. Kim, S.W. Lee, H. Chen, *Microstructural evolution and electrical property of Ta-doped SnO₂ films grown on Al₂O₃ (0001) by metalorganic chemical vapour deposition*, **Thin Solid Films**, **405**, 2002, pp. 256-262.
- [6] P.S. Raghupathi, J. George, C.S. Menon, *Effect of substrate temperature on the electrical and optical properties of reactively evaporated tin oxide thin films*, **Indian Journal of Pure and Applied Physics**, **43**, 2015, pp. 620-623.
- [7] M. Weidner, J. Brotz, A. Klein, *Sputtered deposited polycrystalline tantalum-doped SnO₂ layers*, **Thin Solid Films**, **555**, 2014, pp. 173-178.
- [8] Y. Yin, S. Zhou, G. Gu, L. Wu, *Preparation and properties of uv-curable polymer/nanosized indium-doped tin oxide (ITO) nanocomposite coatings*, **Journal of Materials Science**, **42**, 2007, pp. 5959-5963.
- [9] M.A. Aouaj, R. Diaz, A. Belayachi, F. Rueda, M. Abd-Lefdil, *Comparative study of ITO and FTO thin films grown by spray pyrolysis*, **Materials Research Bulletin**, **44**, 2009, pp. 1458-1461.
- [10] S.M.A. Durrani, M.F.A. Al-Kuhaili, I.A. Bakhtiari, M.B. Haider, *Investigation of the carbon monoxide gas sensing characteristics of tin oxide mixed cerium oxide thin films*, **Sensors**, **12**, 2012, pp. 2598-2909.
- [11] C.K. Kim, S.M. Choi, I.H. Noh, J.H. Lee, C.Hong, H.B. Chae, G.E. Jang, H.D. Park, *A study on thin film gas sensor based on SnO₂ prepared by pulsed laser deposition method*, **Sensors and Actuators B**, **77**, 2001, pp. 463-467.

- [12] S.W. Lee, Y.W. Kim, H. Chen, *Electrical properties of Ta-doped SnO₂ thin films prepared by the metal-organic chemical vapor deposition method*, **Applied Physics Letters**, **78**, 2001, pp. 350-352.
- [13] J. Xu, S. Huang, Z. Wanga, *First principle study on the electronic structure of fluorine doped SnO₂*, **Solid State Communications**, **149**, 2009, pp. 527-531.
- [14] M.M. Hamasha, T. Dhakal, K. Alzoubi, S. Albahri, A. Qasaimah, S. Lu, C.R. Westgate, *Stability of ITO thin film on flexible substrate under thermal aging and thermal cycling conditions*, **Journal of Display Technology**, **8**, 2012, pp. 385-390.
- [15] T. Minami, S. Tsukada, Y. Minamino, T. Miyata, *Preparation of transparent and conductive multicomponent Zn-In-Sn oxide thin films by vacuum arc plasma evaporation*, **Journal of Vacuum Science Technology A**, **23**, 2005, pp. 1128-1132.
- [16] Y. Hayashi, K. Kondo, K. Murai, T. Moriga, I. Nakabayashi, H. Fukumoto, K. Tominaga, *ZnO-SnO₂ transparent conductive films deposited by opposed target sputtering system of ZnO and SnO₂ targets*, **Vacuum**, **74**, 2004, pp. 607-611.
- [17] D.L. Young, D.L. Williamson, T.J. Coutts, *Structural characterization of zinc stannate thin films*, **Journal of Applied Physics**, **91**, 2002, pp. 1464-1471.
- [18] T. Minami, *New n-type transparent conducting oxides*, **Materials Research Society Bulletin**, **25**, 2000, pp. 38-44.
- [19] B. Stjema, E. Olsson, *Optical and electrical properties of radio frequency sputtered tin oxide films doped with oxygen vacancies, F, Sb, or Mo*, **Journal of Applied Physics**, **76**, 1994, pp. 3797-3817.
- [20] Y. Wang, T. Brezesinski, M. Antonietti, B. Smarsly, *Ordered mesoporous Sb-, Nb-, and Ta-doped SnO₂ thin films with adjustable doping levels and high electrical conductivity*, **ACS Nano**, **3**, 2009, pp. 1373-1378.
- [21] I.H. Ko, I.H. Kim, D. Kim, K.S. Lee, T.S. Lee, I.H. Jeong, B. Cheong, Y.I. Baik, W.M. Kim, *Effect of ZnO addition on electrical and structural properties of amorphous SnO₂ thin films*, **Thin Solid Films**, **494**, 2006, pp. 42-46.
- [22] S. Nakao, N. Yamada, T. Hitosugi, Y. Hirose, T. Shimada, T. Hasegawa, *High mobility exceeding 80 cm²V⁻¹S⁻¹ in polycrystalline Ta-doped SnO₂ thin films on glass using anatase TiO₂ seed layers*, **Applied Physics Express**, **3**, 2010, pp. 031102
- [23] S. Nakao, N. Yamada, T. Hitosugi, Y. Hirose, T. Shimada, T. Hasegawa, *Fabrication of highly conductive Ta-doped SnO₂ polycrystalline films on glass using seed-layer technique by pulse laser deposition*, **Thin Solid Films**, **518**, pp. 3093-3096.
- [24] N. Yamada, S. Nakao, T. Hitosugi, T. Hasegawa, *Sputtered deposition of high-mobility Sn_{1-x}Ta_xO₂ films on anatase-TiO₂-coated glass*, **Japanese Journal of Applied Physics**, **49**, 2010, pp. 108002.
- [25] C.U. Mordi, M.A. Eleruja, B.A. Taleatu, G.O. Egharevba, A.V. Adedeji, O.O. Akinwunmi, B. Olofinjana, C. Jeynes, E.O.B. Ajayi, *Metal organic chemical vapour deposited thin films of cobalt oxide prepared via cobalt acetylacetonate*, **Journal of Materials Science and Technology**, **25**, 2009, pp. 85-89.
- [26] O. Fasakin, M.A. Eleruja, O.O. Akinwunmi, B. Olofinjana, E. Ajenifuja, E.O.B. Ajayi, *Synthesis and characterization of metal organic chemical vapour deposited copper titanium oxide (Cu-Ti-O) thin films from single solid source precursor*, **Journal of Modern Physics**, **4**, 2013, pp. 1-6.
- [27] K.O. Oyedotun, M.A. Eleruja, B. Olofinjana, O.O. Akinwunmi, O.O. Ilori, E. Omotoso, E. Ajenifuja, A.T. Famojuro, E.I. Obianjuwa, E.O.B. Ajayi, *Some properties of manganese oxide (Mn-O) and lithium manganese oxide (Li-Mn-O) thin films prepared via metal*

- organic chemical vapor deposition (MOCVD) technique*, **Journal of Materials Science and Engineering B**, **5**, 2015, pp. 231-242.
- [28] S.F. Tayyari, F. Milani-nejad, *Vibrational assignment of acetylacetonate*, **Spectrochimica Acta Part A: Molecular and Biomolecular Spectroscopy**, **56**, 2000, pp. 2679-2691.
- [29] Y. Muto, S. Nakatomi, N. Oka, Y. Iwabuchi, H. Kotsubo, Y. Shigestato, *High rate deposition of Ta-doped SnO₂ films by reactive magnetron sputtering using a Sn-Ta metal-sintered target*, **Thin Solid Films**, **520**, 2012, pp. 3746-3750.
- [30] D. Raoufi, A. Kiasatpour, H.R. Fallah, A.S.H. Rozataian, *Surface characterization and microstructure of ITO thin films at different annealing temperature*, **Applied Surface Science**, **253**, 2007, pp. 9085-9090.
- [31] S. Ezhilvalavan, T.Y. Tseng, *Short duration rapid-thermal-annealing processing of tantalum oxide thin films*, **Journal of the American Ceramic Society**, **82**, 1999, pp. 600-606.
- [32] K.Y. Rajpure, M.N. Kusumade, M.N. Neumann-Spallart, CH. Bhosale, *Effect of Sb doping on properties of conductive spray SnO₂ thin film*, **Materials Chemistry and Physics**, **64**, 2000, pp. 184-188.
- [33] S.V. Jagadeesh, S. Uthanna, G. Mohan Rao, *Effect of substrate temperature on the structural, optical and electrical properties of dc magnetron sputtered tantalum oxide films*, **Applied Surface Science**, **254**, 2008, pp. 1953-1960.
- [34] M.S. Hossain, H. Kabir, M.M. Rahman, K. Hasan, M.S. Bashar, M. Rahman, M.A. Gafur, S. Islam, A. Amri, Z.T. Jiang, M. Altarawneh, B.Z. Dlugogorski, *Understanding the shrinkage of optical absorption edges of nanostructured Cd-Zn Sulphide films for photothermal applications*, **Applied Surface Science**, **392**, 2017, pp. 854-862.
- [35] Y.G. Wang, S.P. Lau, H.W. Lee, S.F. Yu, B.K. Tay, X.H. Zhang, H.H. Hong, *Photoluminescence study of ZnO films prepared by thermal oxidation of ZnO metallic films in air*, **Journal of Applied Physics**, **94**, 2003, pp. 354-358.
- [36] D.K. Schroeder, **Semiconductor materials and device characterizations** (second edition), Wiley-Interscience Publication, Arizona, 1998, pp. 14-17.
- [37] G. Kiriakidis, M. Bender, N. Katsarakis, E. Gagaoudakis, E. Hourdakis, E. Douloufakis, V. Cimalla, *Ozone sensing properties of polycrystalline indium oxide films at room temperature*, **Physica Status Solidi A**, **185**, 2001, pp. 27-32.

Received: August 10, 2017

Accepted: September 10, 2017